NASA CONTRACTOR REPORT

NASA CR-2325

NASA CR-2325

THE METEOROLOGICAL EFFECTS ON MICROWAVE APPARENT TEMPERATURES LOOKING DOWNWARD OVER A SMOOTH SEA

by Steve Wu

Prepared by

THE UNIVERSITY OF KANSAS CENTER FOR RESEARCH, INC.

Lawrence, Kans. 66044

for Langley Research Center

NATIONAL AERONAUTICS AND SPACE ADMINISTRATION • WASHINGTON, D. C. • NOVEMBER 1973

1. Report No.	2. Government Accession No.	3. Recipient's Catalog No.
NASA CR-2325		

4. Title and Subtitle	5. Report Date
The Meteorological Effects on Microwave Apparent Temperatures Looking Downward over a Smooth Sea	November 1973
	6. Performing Organization Code
7. Author(s) Steve Wu	8. Performing Organization Report No. TR 186-1
9. Performing Organization Name and Address The University of Kansas Center for Research, Inc. 2291 Irving Hill Road - Campus West Lawrence, Kansas 66044	10. Work Unit No.
	11. Contract or Grant No. NAS 1-10048
	13. Type of Report and Period Covered Contractor Report
12. Sponsoring Agency Name and Address National Aeronautics and Space Administration Washington, D. C. 20546	14. Sponsoring Agency Code

15. Supplementary Notes

This is a topical report.

16. Abstract

The effects of clouds and rain on microwave apparent temperatures for a flat sea surface are examined. The presence of clouds and rain can be expressed as a change of absorption coefficient and the total absorption is computed as the sum of individual effects.

Various cloud and rain models proposed by meteorologists are employed to compute the microwave apparent temperature when viewing downward through these model atmospheres. It is shown that stratus, cumulus, overcast, and rain all contribute significantly to the observed temperature. Larger sensitivities to clouds and rain are observed for horizontally polarized apparent temperature at large nadir angles than for vertically polarized apparent temperature.

17. Key Words (Selected by Author(s))	18. Distribution Statement
apparent temperature clouds or rain model absorption coefficient	Unclassified - Unlimited

19. Security Classif. (of this report)	20. Security Classif. (of this page)	21. No. of Pages	22. Price*
Unclassified	Unclassified	37	Domestic, $3.00 Foreign, $5.50

*For sale by the National Technical Information Service, Springfield, Virginia 22151

FOREWORD

This document reports the meteorological effects on microwave apparent temperatures looking downward over a smooth sea. This work was performed by the University of Kansas during the first year of a joint program (RADSCAT) with New York University, General Electric Space Division, and NASA Langley Research Center. This study was performed under Contract NAS 1-10048, issued by the NASA Advanced Applications Flight Experiments Office, Langley Research Center, Hampton, Virginia.

TABLE OF CONTENTS

THE METEOROLOGICAL EFFECTS ON MICROWAVE APPARENT TEMPERATURES LOOKING DOWNWARD OVER A SMOOTH SEA

I. INTRODUCTION

The first theoretical study of the apparent temperature of the rough sea surface at microwave frequencies was by Stogryn [1967].[1] Fung and Ulaby [1969] using a physical optics approach also calculated the effect of surface roughness on the apparent surface temperature. In all these studies, the atmosphere above the sea surface is assumed to be ARDC standard.[3]

None of the above works considers the effects of rain or cloud. Since these effects may be present a good percentage of the time, for instance, during sea state mapping with satellites, it is the purpose of this work to examine the meteorological effects on microwave apparent temperatures for a flat sea surface.

II. THE APPARENT TEMPERATURE AND SURFACE EMISSIVITY OF A SMOOTH SEA

A. The Apparent Temperature

In order to examine the meteorological effects, the sea surface is assumed flat. The apparent temperature at height, H, can be expressed as:

$$T_{aj}(\theta) = L(\theta)\left[\epsilon_j(\theta)\, T_G + (1-\epsilon_j(\theta))\, T_{sky}(\theta)\right] + T_{atm}(\theta) \qquad (1)$$

where

θ = is the nadir angle

j = h or v, is for horizontal or vertical polarization of measured temperatures.

$L(\theta)$ = the transmittance of the atmosphere at height H

$$= \text{Exp}\left(-\sec\theta \int_0^H \alpha(z)\, dz\right) \qquad (2)$$

T_a = sea surface temperature °K

$T_{sky}(\theta)$ = the sky temperature of the atmosphere

$$= \sec\theta \int_0^\infty T(z')\alpha(z')\, e^{-\sec\theta \int_0^{z'} \alpha(z)dz} dz' \qquad (3)$$

$T_{atm}(\theta)$ = the apparent temperature due to the atmosphere between the surface and the height H

$$= \sec\theta \int_0^H T(z')\alpha(z') e^{-\sec\theta \int_{z'}^H \alpha(z)dz} dz' \qquad (4)$$

In equations (2), (3), and (4), T(z) is the thermometric temperature, $\alpha(z)$ is the total absorption coefficient of the atmosphere at height z to be specified in the next section.

Since the angle of incidence is equal to the angle of reflection for a flat surface, the apparent temperature, the sky temperature and the atmospheric temperature calculated up to a height H are functions of Θ only.

B. The Surface Emissivity

In equation (1), $\epsilon_j(\theta)$ is the surface emissivity related to the Fresnel reflection coefficient for a flat surface by:

$$\epsilon_j(\theta) = 1 - |R_j(\theta)|^2 \qquad j = h \quad \text{or} \quad V \qquad (5)$$

and $R_h(\theta)$ = horizontal Fresnel reflection coefficient

$$= \frac{\cos\theta - \sqrt{\epsilon_r - \sin^2\theta}}{\cos\theta + \sqrt{\epsilon_r - \sin^2\theta}} \qquad (6)$$

$R_v(\theta)$ = vertical Fresnel reflection coefficient

$$= \frac{\epsilon_r \cos\theta - \sqrt{\epsilon_r - \sin^2\theta}}{\epsilon_r \cos\theta + \sqrt{\epsilon_r - \sin^2\theta}} \qquad (7)$$

In equations (5), (6), and (7), Θ is the angle of incidence, ϵ_r is the complex relative dielectric constant of sea water. ϵ_r at microwave frequencies is given by

$$\epsilon_r = \epsilon_1 - j\,\epsilon_2 = \frac{\epsilon_o - \epsilon_\infty}{1 + j\,\frac{\Delta\lambda}{\lambda}} + \epsilon_\infty \tag{8}$$

From (8) equating the real and the imaginary parts respectively we get

$$\epsilon_1 = \frac{\epsilon_o + \epsilon_\infty \left(\frac{\Delta\lambda}{\lambda}\right)^2}{1 + \left(\frac{\Delta\lambda}{\lambda}\right)^2} \tag{9}$$

$$\epsilon_2 = \frac{\left(\epsilon_\infty - \epsilon_o\right)\left(\frac{\Delta\lambda}{\lambda}\right)}{1 + \left(\frac{\Delta\lambda}{\lambda}\right)^2} \tag{10}$$

In (9) and (10), $\epsilon_\infty = 5.5$, λ is the wavelength in cm. The static dielectric constant ϵ_o and the relaxation wavelength $\Delta\lambda$ are functions of sea water temperature, T_G, and can be expressed in terms of an interpolation polynomial[1].

$$\epsilon_o = 87.7 - 0.4008\,(T_G - 273) + 9.398 \times 10^{-4}(T_G - 273)^2 - 1.410 \times 10^{-6}(T_G - 273)^3 \tag{11}$$

$$\Delta\lambda = 3.33 - 0.1122\,(T_G - 273) + 1.8 \times 10^{-3}(T_G - 273)^2 - 8.3 \times 10^{-6}(T_G - 273)^3 \quad \text{CM} \tag{12}$$

It is possible to calculate the surface emissivity using (6), (7), and (5), but with a complex dielectric constant under the square root sign, direct substitution leads easily to erroneous results. Hence, it is necessary to rearrange the expression for surface emissivity. (The detailed derivation is shown in appendix A)

$$\epsilon_h(\theta) = \frac{4B\cos\theta\cos\psi_o}{F_1} \tag{13}$$

$$\epsilon_v(\theta) = \frac{4GB\cos(\psi_2 - \psi_0)}{F_2} \tag{14}$$

where

$$B = \left[(\epsilon_1 - \sin^2\theta)^2 + \epsilon_2^2\right]^{1/4} \tag{15}$$

$$\psi_0 = \frac{1}{2}\tan^{-1}\left(\frac{\epsilon_2}{\epsilon_1 - \sin^2\theta}\right) \tag{16}$$

$$F_1 = \cos^2\theta + 2B\cos\theta\cos\psi_0 + B^2 \tag{17}$$

$$\psi_2 = \tan^{-1}\left(\frac{\epsilon_2}{\epsilon_1}\right) \tag{18}$$

$$G = \cos\theta\,(\epsilon_1^2 + \epsilon_2^2)^{1/2} \tag{19}$$

$$F_2 = G^2 + B^2 + 2GB\cos(\psi_2 - \psi_0) \tag{20}$$

III. ABSORPTION COEFFICIENTS OF OXYGEN, WATER VAPOR, CLOUD AND RAIN (UNDER LOCAL THERMODYNAMIC EQUILIBRIUM AND IGNORING THE SCATTERING EFFECTS)

The meteorological variation of the atmosphere due to the presence of clouds and rains can be expressed as a change of the absorption coefficient. Other weather conditions such as snow and hail or thunderstorm will not be considered here. The total emission or absorption is computed as the sum of individual effects. Hence, it is convenient to consider each effect in turn.

A. Clear Sky Model Atmosphere and Absorption Coefficient

For clear sky at microwave frequencies the main absorption is due to molecular oxygen and water vapor, and the absorption coefficient is a function of temperature, pressure and water vapor density of the atmosphere. Hence it is necessary to specify the atmospheric conditions. One possible specification is as follows:[3]

Temperature

$$T(z) = T_G - \frac{7}{11} z \quad {}^\circ K \quad \text{for} \quad z \leq 11 \text{ KM}$$

$$= 217 \quad {}^\circ K \quad \text{for} \quad z > 11 \text{ KM} \tag{21}$$

where T_G = sea surface temperature

z = the height in km above mean sea level

Pressure

$$P(z) = P_G \, e^{-0.143 z} \quad \text{mm Hg} \tag{22}$$

$$P_a = \frac{1013.25}{760} P(z) \quad \text{millibar} \tag{23}$$

where P_G = sea surface pressure in mm Hg

P_a = absolute pressure in millibar

Water vapor density

$$\rho(z) = \rho_G \, e^{-z/2.2} \quad \text{gm/m}^3 \tag{24}$$

where ρ_G = sea surface water vapor density in gm/m^3

The absorption of molecular oxygen and water vapor has been studied extensively since van Vleck and Weisskopf [1945][4]. Formulas for computing the absorption coefficient can be found elsewhere [Porter, 1970].[18] The following equations for oxygen and water vapor absorption are adopted for this work.

Molecular Oxygen

There are two line width parameters for oxygen at microwave frequencies. The 60 GHz complex and the 118.75 GHz line are obtained from Meeks and Lilley [1963]:[5]

$$\alpha_{60}(z) = C K_{60} \gamma_{60} \left[\frac{1}{(60-\nu)^2 + \Delta\nu^2} + \frac{1}{(60+\nu)^2 + \Delta\nu^2} + \frac{1}{\nu^2 + \Delta\nu^2} \right] \tag{25}$$

where $\alpha_{60}(z)$ = Absorption coefficient of 60 GHz complex at z in neper/km

ν = propagating frequency in GHz

$\Delta\nu$ = line width factor in GHz

$$= 1.5 \left(\frac{T_G}{T(z)}\right)^{1/2} \left(\frac{P(z)}{P_G}\right) \tag{26}$$

$$\gamma_{60} = 0.21\, \Delta\nu\, P(z)\, \nu^2 / T(z)^3 \tag{27}$$

$CK_{60} = 362.6$

$T(z)$, T_G, $P(z)$, P_G are specified in equations (21) and (22).

$$\alpha_{118}(z) = C K_{118} \gamma_{118} \left[\frac{1}{(118.75-\nu)^2+\Delta\nu^2} + \frac{1}{(118.75+\nu)^2+\Delta\nu^2}\right] \tag{28}$$

where

$\alpha_{118}(z)$ = Absorption Coefficient of 118.75 GHz line at z in neper/km

$CK_{118} = 5.23$

$\gamma_{118} = \gamma_{60}$ $\Delta\nu$, ν are defined as the same in $\alpha_{60}(z)$ case.

Water Vapor

There are three parts for water vapor absorption coefficient. The 22,235 GHz absorption line and the residual absorption were calculated according to Barret and Chung [1962].[6] The millimeter absorption line at 183.3 GHz was obtained from Ulaby and Straiton [1970]:[7]

$$\alpha_{22}(z) = C K_{22} \gamma_{22} \left[\frac{1}{(\nu-22.235)^2+\Delta\nu^2} + \frac{1}{(\nu+22.235)^2+\Delta\nu^2}\right] \tag{29}$$

where $\alpha_{22}(z)$ = Absorption coefficient of 22,235 GHz line at z in neper/km

ν = propagating frequency in GHz

$$\Delta\nu = 2.58 \times 10^{-3} P_a \left(1 + 0.0147 \rho(z) T(z)/P_a\right)\left(\frac{318}{T(z)}\right)^{.625} \text{ GHz} \quad (30)$$

$$\gamma_{22} = e^{-644/T(z)} \nu^2 P_a P(z) \left(1 + 0.0147 \rho(z) T(z)/P_a\right) T(z)^{-3.125} \quad (31)$$

$$CK_{22} = 32.4$$

$$\alpha_{RES}(z) = CK_{RES}\, \rho(z)\, \nu^2 \Delta\nu / T(z)^{1.5} \quad (32)$$

where $\alpha_{RES}(z)$ = Absorption coefficient of the residual lines at z in neper/km

$CK_{RES} = 2.55 \times 10^{-3}$

$\Delta\nu$ is the same as in equation (30)

$$\alpha_{183}(z) = CK_{183}\, \gamma_{183}\left[\frac{1}{(\nu - 183.31)^2 + \Delta\nu^2} + \frac{1}{(\nu + 183.31)^2 + \Delta\nu^2}\right] \quad (33)$$

where

$\alpha_{183}(z)$ = Absorption coefficient of 183.3 GHz line at z in neper/km

$$\Delta\nu = 3.0 \left(\frac{P(z)}{760}\right)\left(\frac{290}{T(z)}\right)^{1/2} \quad (34)$$

$$\gamma_{183} = \rho(z)\, \Delta\nu \left(\frac{290}{T(z)}\right)^2 \nu^2 \times 1/3 \quad (35)$$

$$CK_{183} = 8.6 \times 10^{-3}$$

The clear sky absorption coefficient for frequency, ν, and height, z, is the sum of oxygen and water vapor absorption coefficients. It is expressed as:

$$\alpha_{CS}(z) = \alpha_{60}(z) + \alpha_{118}(z) + \alpha_{22}(z) + \alpha_{RES}(z) + \alpha_{183}(z) \quad (36)$$

Pressure, temperature and water vapor density of the atmosphere decrease with increasing altitude. Hence, the clear sky absorption coefficient also decreases with increasing altitude as shown in equations (25) through (35).

B. Cloudy or rainy sky model atmosphere and absorption coefficient

The presence of clouds and rain can be expressed as a change of absorption coefficient. Even though we have information on the absorption coefficient for a given liquid water content of the clouds and precipitation rate, computation of total absorption or emission depends on selecting a meteorologically sound model for the clouds and rain.

(a) Cloud model

According to meteorological classification[20] there are three basic cloud forms namely cirrus, cumulus and stratus. All the other standard types are either these pure forms or modifications and combinations of them at different elevations, where varying air and moisture conditions are responsible for their form.

Since cirrus clouds normally stay above 30,000 ft. and are thin layers of ice, their effect on attenuation is relatively small compared with other types of clouds. Thus only the effects of cumulus and stratus clouds are considered in this work. Refering to Malkus[21], Spyers-Duran[22] and Levine[23], it is appropriate to use Levine's classification for cumulus clouds:

Case 1	457^m	$\leq$	z	$\leq$	1068^m	,	M = 0.5	gm/m^3
Case 2	457^m	$\leq$	z	$\leq$	2590^m	,	M = 1.0	gm/m^3
Case 3	457^m	$\leq$	z	$\leq$	3810^m	,	M = 1.25	gm/m^3

Usually the liquid water content of the cloud varies with height and attains its maximum near the cloud top. The data listed above are the average value over total cloud thickness. For stratus cloud Neiburger's[24] investigation is consistent with Aufm Kampfe and Weickmann[25] and is quoted below:

Case I	30^m	$\leq$	z	$\leq$	580^m	M= 0.35 gm/m^3
Case II	152^m	$\leq$	z	$\leq$	520^m	M= 0.25 gm/m^3
Case III	213^m	$\leq$	z	$\leq$	490^m	M= 0.20 gm/m^3

Porter's[1970][18] classification of overcast can be considered as a combination of stratus and cumulus clouds:

Light overcast (sun image visible)

$300^m \leq z \leq 650^m$ M=0.33 gm/m^3

Medium overcast (no sun, light sky)

$400^m \leq z \leq 900^m$ M=0.67 gm/m^3

Heavy overcast

$500^m \leq z \leq 3200^m$ M=1.0 gm/m^3

Kreiss[1968][15] also classified the clouds in stratus, thick stratus, and tall cumulus cloud with different liquid water content ranging from 0.0625 gm/m^3 to 4 gm/m^3. Without considering the possible range of liquid water content for a specific cloud type, his models are not so well defined as the others:

Stratus cloud

$628^m \leq z \leq 1457^m$ M=0.0625,.25,.5,1,2,4 gm/m^3

$628^m \leq z \leq 1949^m$ M=0.0625,0.125,0.25,0.5,1,2,4 gm/m^3

Thick stratus cloud

$628^m \leq z \leq 3012^m$ M=0.0625,0.125,0.25,0.5,1,2,4 gm/m^3

Tall cumulus cloud

$628^m \leq z \leq 7185^m$ M=0.0625,0.125,0.25,0.5,1,4 gm/m^3

(b) Rain model

Statistics are available for most parts of the world to give the average monthly precipitation but data on precipitation rates are scarce. Furthermore, although many stations give distributions of precipitation rates, these are for single locations, and little informations is available on the horizontal extent of precipitation of differing intensities - particularly over the ocean. Valley's[1965][3] classification, which is reasonably complete for moderate rain, is quoted for this work:

Case I is representative of summer rain in temperate latitudes and with a slight increase of temperature, of wide-spread tropical rains as well. Precipitation distribution is shown in Figure 1 and 2.

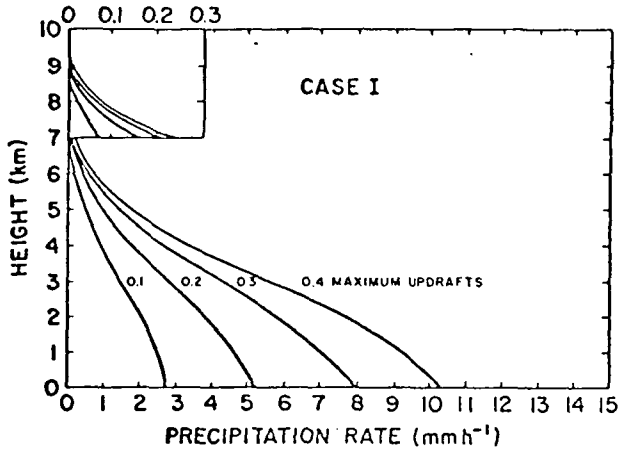

Fig. 1. Distribution of precipitation rate with altitude for Case I. Values of maximum updraft in m sec^{-1} are given by each curve.

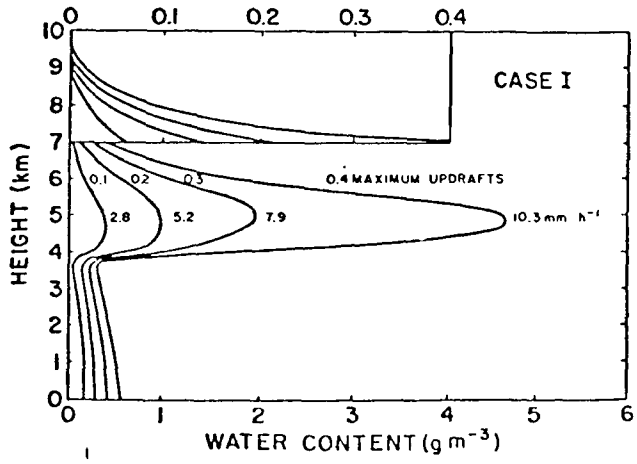

Fig. 2. Concentration of precipitation, in g m^{-3}, with height for Case I. Values of maximum updraft in m sec^{-1} (above) and surface precipitation rate in mm h^{-1} (below) are given by each curve.

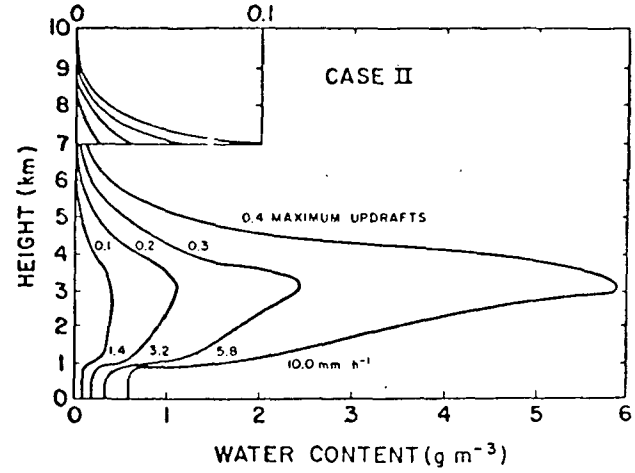

Fig. 3. Concentration of precipitation, in g m^{-3}, with height, for Case II. Values of maximum updraft in m sec^{-1} (above) and surface precipitation rate in mm h^{-1} (below) are shown by each curve.

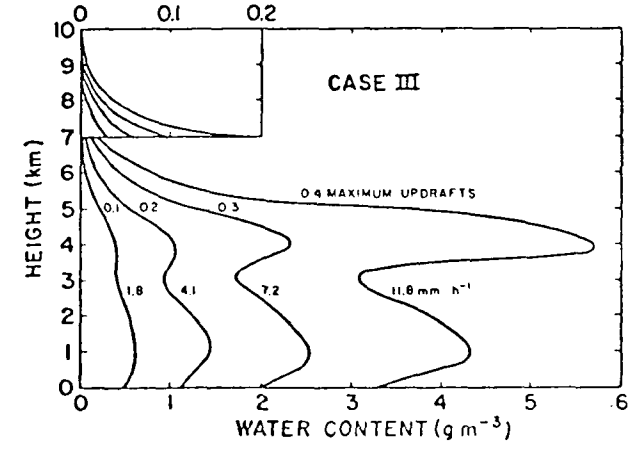

Fig. 4. Concentration of precipitation in g m^{-3}, with height, for Case III. Values of maximum updraft in m sec^{-1} (above) and surface precipitation rate in mm h^{-1} (below) are shown by each curve.

Case II is associated with rain in the spring and fall months in temperate latitudes and also represents a likely thermal stratification during much orographic rain in temperate climes.

Case III patterned after the atmospheric structure during severe snow storms in New England, is representative of a winter snowstorms and except for the low temperatures, characterizes the winter rains as well.

All cases pertain to widespread uniform precipitation, not to showery conditions. The concentration of precipitation for case II and III is shown in Figure 3 and 4.

Due to different updrafts, four different precipitation rates exist for each case. The precipitation rate for case I, together with cloud cover above the precipitation is listed as follows:

(1) 0.4 m/sec updraft							
	rain	0	$\leq$	z	$\leq$	3100^m	p=10.3 mm/hr
	cloud	3100	$\leq$	z	$\leq$	7000^m	M=0.3 gm/m^3
(2) 0.3 m/sec updraft							
	rain	0	$\leq$	z	$\leq$	3200^m	p=7.9 mm/hr
	cloud	3200	$\leq$	z	$\leq$	7000^m	M=0.25 gm/m^3
(3) 0.2 m/sec updraft							
	rain	0	$\leq$	z	$\leq$	3300^m	p=5.2 mm/hr
	cloud	3300	$\leq$	z	$\leq$	7000^m	M=0.15 gm/m^3
(4) 0.1 m/sec updraft							
	rain	0	$\leq$	z	$\leq$	3500^m	p=2.8 mm/hr
	cloud	3500	$\leq$	z	$\leq$	7000^m	M=0.1 gm/m^3

Both precipitation rate and liquid water content vary with altitude. The data shown are the average value of precipitation and cloud layer.

The above mentioned models for clouds and rain may be a gross simplification of the real situation in many ways, they form a basis for calculating the meteorological effects on apparent temperature to be discussed in the next section.

The absorption coefficient of clouds and rain can be calculated by Mie's theory [1908].[19] The extinction cross-section for single drop is

given as:

$$Q_{ex} = -\frac{\lambda^2}{2\pi} R_e \sum_{n=1}^{\infty} (2n+1)(a_n^s + b_n^s) \qquad (37)$$

where λ is the wavelength and a_n^s, and b_n^s are functions of spherical Bessel functions with complex dielectric constant and radius of water drop as an argument. The complex dielectric constant of water at microwave frequency varies with temperature; hence the extinction cross-section is temperature and frequency dependent.

Ryde and Ryde[1946][8] were the first to calculate the attenuation of clouds and rain based on Mie's theory, and their result has been the basis for much of the subsequent works. By using Laws and Parsons drop-size distribution of various precipitation rates, they calculated the theoretical attenuation coefficient of rain directly in terms of eight different precipitation rates with eight wavelengths from 0.3 to 10 cm at 18°C. For temperature different from 18°C, the correction factor is tabulated from 0 to 40°C at 10°C interval.

For non-precipitating clouds with drop radii much less than the wavelength, the familiar Rayleigh scattering equation was used by Goldstein[1951][13] to calculate cloud attenuation.

Gunn and East[1954][9] not only reviewed Ryde's development since 1946, but added the backscattering cross section calculation for clouds and rain which has been widely quoted in radar meteorology. The dielectric constant of ice is very much different from water. Consequently they calculated the attenuation of ice and water clouds separately, and the temperature effect was also included.

Medhurst[1965][12], using Ryde's theoretical approach, re-calculated the attenuation for rain with five precipitation rates and sixteen wavelengths from 0.3 to 15 cm at 20°C. He also collected rain attenuation measurements from 1946 to 1962, and compared with his theoretical result. He used a set of theoretical maximum and minimum attenuations for rain to compare with measurements and concluded that the agreement was not entirely satisfactory.

There was a tendency for measured attenuation to exceed the maximum possible levels predicted by the theory. But recent measurements by Brown and Haroules[1969][14] at 8 GHz and 15 GHz indicate that there is no tendency for measured attenuations to lie above the theoretical maximum values. Hence theoretical calculations seem to provide a reasonable basis for the prediction of attenuation by rain.

(c) Clouds absorption coefficient

In this work, Benoit's[1968][10] equations for water and ice clouds were used to calculate the cloud attenuation. Although he did not shed any new light on basic theoretical calculations, his effort to interpolate Gunn and East's discrete data with respect to frequency and temperature and to come out with one simple empirical equation[15] very convenient for computation purpose, particularly when the temperature varies continuously with respect to height in the atmosphere.

The absorption coefficient for clouds can be expressed as:[10]

$$\alpha_c(z) = M \nu^b e^a \qquad dB/Km \tag{38}$$

where

M = liquid water content of clouds in gm/m^3

ν = propagating frequency in GHz

b = frequency index, for water cloud $b_w = 1.95$

frequency index, for ICE cloud $b_i = 1.006$

a = temperature coefficient

$a_w = -6.866\ (1+.0045t)$

$a_i = -8.261\ (1-1.767 \times 10^{-2} t - 4.374 \times 10^{-4} t^2)$

and t is temperature in °c and varies with respect to height z. That is t=f(z).

Figure 5 shows Gunn and East's original discrete data and the straight lines were drawn by Benoit using the interpolating equation (38).

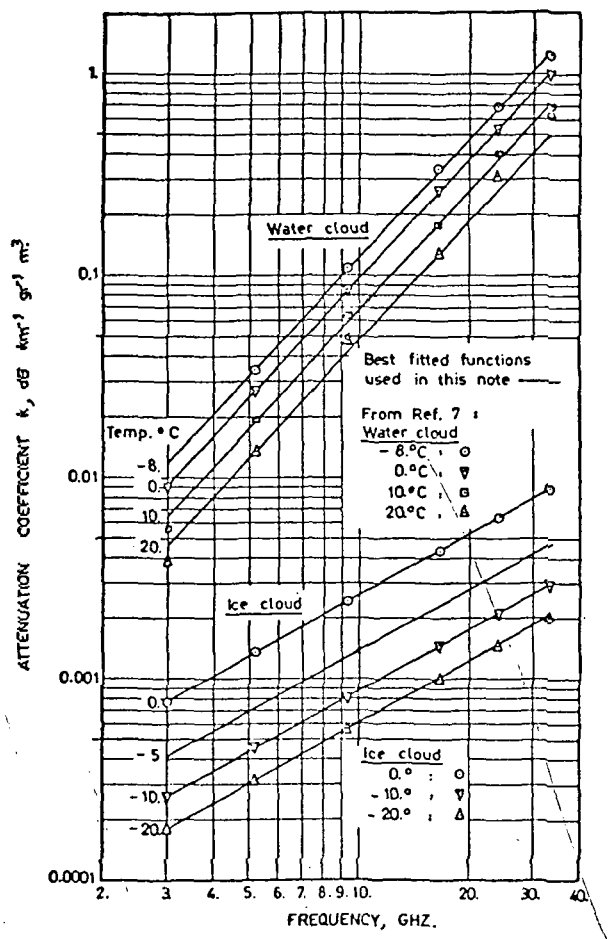

Fig. 5 — Attenuation coefficient for clouds.

(d) Rain absorption coefficient

Presently available absorption coefficients for rain are all expressed in terms of attenuation in db/km; if the scattering effect is ignored, the attenuation is mainly due to absorption and we can use attenuation coefficient to calculate apparent temperature. Although rain drops are much larger than water drops in clouds(we can ignore scattering effect for cloud), for this study we will assume scattering can be ignored.

A future study will include this scattering effect in detail for various rain conditions. Here we use Gunn and East's empirical expression:

$$\alpha_R = a p^b \tag{39}$$

to relate the attenuation to the precipitation rate. α_R is the attenuation in db/km and p is the precipitation rate in mm/hr. The parameters a and b are frequency dependent constants. Refering to Ippolito[1970][26], the a and b parameters are obtained with Laws and Parson's distribution at three frequencies of interest as:

a=0.008	b=1.32	at 8.9 GHz
a=0.0125	b=1.25	at 11.1 GHz
a=0.026	b=1.18	at 13.9 GHz

Ippolito has shown that the attenuation calculated by this formula is between Medhurst's[1965] theoretical maximum and minimum attenuation.

IV. CALCULATED RESULTS

In this section, curves of apparent temperature versus nadir angle and frequency are computed using the equations in section II and the atmospheric models of clouds and rain in section III. The calculation is based on local thermodynamic equilibrium with scattering effect ignored.

The purpose of these computations is to determine how well these models agree with experiments. Furthermore, they also serve to indicate the masking effect of clouds or rain on the observation of the areas below them.

For our clear sky apparent temperature calculation, we assumed $T_G = 300°K$, $\rho_G = 9.53$ gm/m^3, $P_G = 760$ mmHg. For clouds or rain, the height of observation is assumed at 10 km. Since the highest cloud top is about 7 km, this would allow various meteorological effects to be examined. For all clouds and rain models, the temperature variation with respect to height, z, is assumed to follow that for the standard atmosphere. The temperature effect on cloud absorption coefficient is included in our apparent temperature calculation. For rain, we assumed constant absorption coefficient throughout the region. The total absorption coefficient then can be expressed as:

$$\alpha_T(z) = \alpha_{cs}(z) + \alpha_{cloud}(t(z)) + \alpha_{rain}(P(z)) \qquad (40)$$

Figure 6 and 7 show curves of apparent temperature versus nadir angle for Porter's overcast models at 13.9 GHz with horizontal and vertical polarization. The clear-sky curves also shown are used as a basis for comparison.

Figure 8 and 9 are the Ta versus θ curves for Neiburger's stratus and Levine's cumulus cloud model at 13.9 GHz with horizontal polarization. Ta versus ν curves at 0 and 60° nadir angle for Levine's cumulus cloud model is shown in Figure 10. The results using Valley's precipitation model case I, with four different precipitation rates, are shown in figures 11 to 13 with Ta vs. θ, Ta vs. ν and Ta vs. P plot.

V. CONCLUSIONS

Presence of clouds and rain will in general increase the microwave apparent temperatures looking downward over a smooth sea. The following conclusions may be made with respect to the cloud and rain models:

(a) Cloud model

(1) Porter's overcast model, which can be considered as a combination of stratus and cumulus cloud models, shows that at 13.9 GHz (Fig 6, and 7) the difference of apparent temperature between any two models at a

given nadir angle increases with increasing nadir angle and attains its maximum value around seventy degrees for horizontal polarization but decreases for vertical polarization. Neiburger's stratus cloud (Figure 8) and Levine's cumulus cloud (Figure 9) models also have the same characteristics.

(2) Due to the above characteristics, it is much easier to use horizontal polarization for cloud detection, particularly at large nadir angles.

(3) Neiburger's stratus cloud model (Figure 8) shows that for thin cloud (500^{m} thick) with average liquid water content less than $0.35\ gm/m^{3}$, the temperature increment is small and its effect can be ignored at 13.9 GHz and below.

(4) The apparent temperature increases at different rates with increasing frequency from 8.9 to 13.9 GHz at a given nadir angle. The increment of a specific model also increases with increasing nadir angle. For example, at nadir, the 3810^{m} cloud top $1.25\ gm/m^{3}$ liquid water content cumulus cloud (see Figure 10) has 27°K variation from 8.9 to 13.9 GHz while at sixty degree nadir angle it increases to 50°K.

(b) Cloud-precipitation model

(1) Valley's precipitation model case I with four different precipitation rates gives results shown in figures 11 to 13. For small precipitation rates, say 2.8 and 5.2 mm/hr, the apparent temperature difference between these two models increases with increasing nadir angle which is the same as shown by the cloud models. For moderate precipitation rates, say 7.9 and 10.3 mm/hr, the apparent temperature difference between these two models does not increase with increasing nadir angle.

(2) The apparent temperature increases at different rates with increasing frequency from 8.9 to 13.9 GHz at nadir and at 60 degree nadir angle for different precipitations (Figure 12). For instance, at nadir the apparent temperature increment from 8.9 to 13.9 GHz for 2.8, 5.2, 7.9 and 10.3 mm/hr models are 18, 26, 34, and 39°K respectively. From this result it is apparent that the larger the precipitation rate the larger the

increments, but there are no linear relations between them. At 8.9 GHz the apparent temperature difference between 10.3 mm/hr and clear sky models is 27°K at nadir, while at 60 degree nadir angle which is twice the path length at nadir, it increases to 60°K (not 54°K). Hence, there is no linear relation between the apparent temperature difference due to rain and the path length of rain though we assumed constant absorption coefficient of rain.

(3) From the above characteristics of moderate rain, these phenomena appear to allow differentiation between cloudy and rainy conditions.

(4) Figure 13 shows the apparent temperature versus precipitation rate curves with three different frequencies. There exists a linear relationship at 8.9 GHz, but at 13.9 GHz, the linearity breaks down around 7.9 mm/hr. Hence, 8.9 GHz may be better for precipitation rate detection by means of apparent temperature measurement.

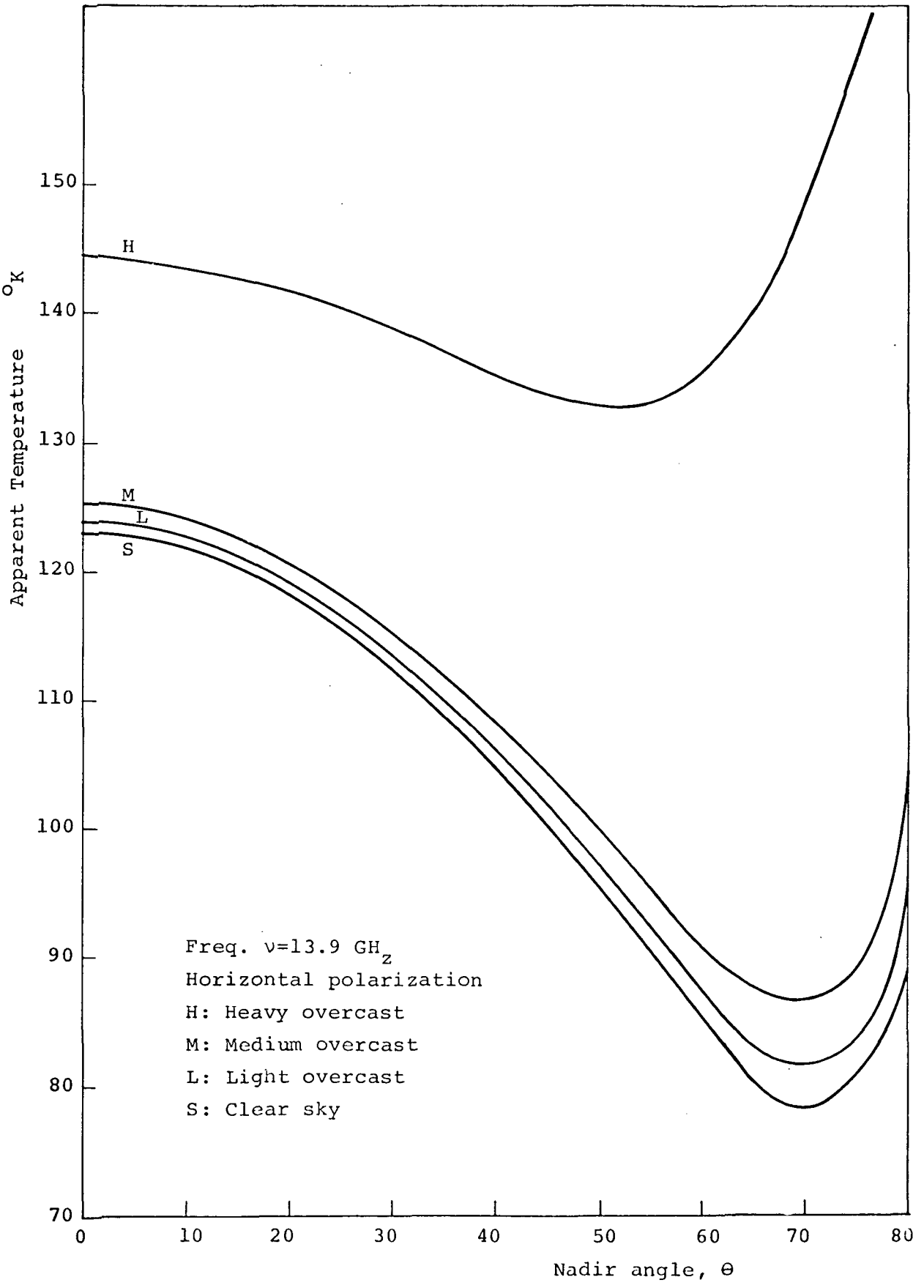

Figure 6. Porter's Overcast Model T_a v.s. θ

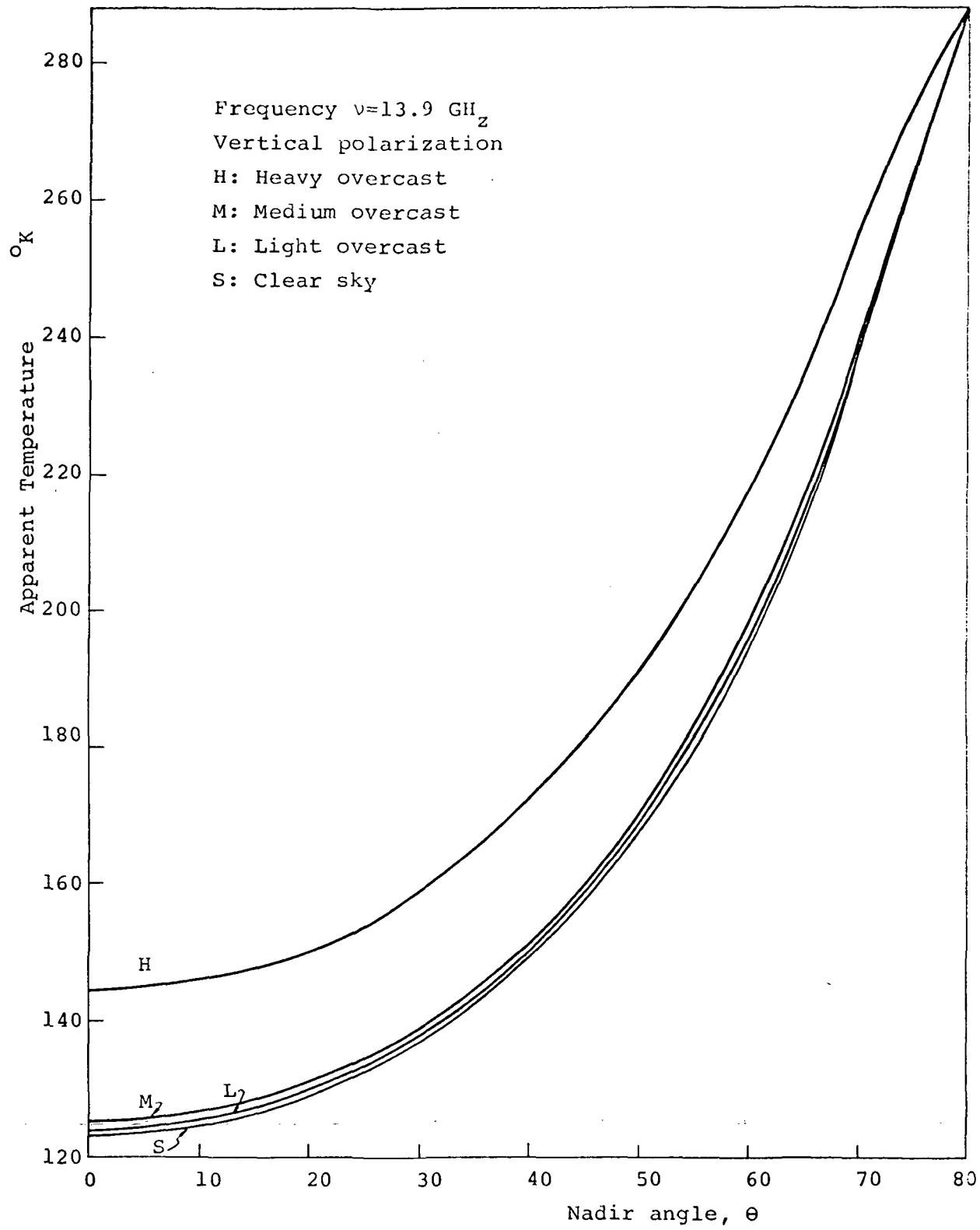

Figure 7. Porter's Overcast Model T_a v.s. θ

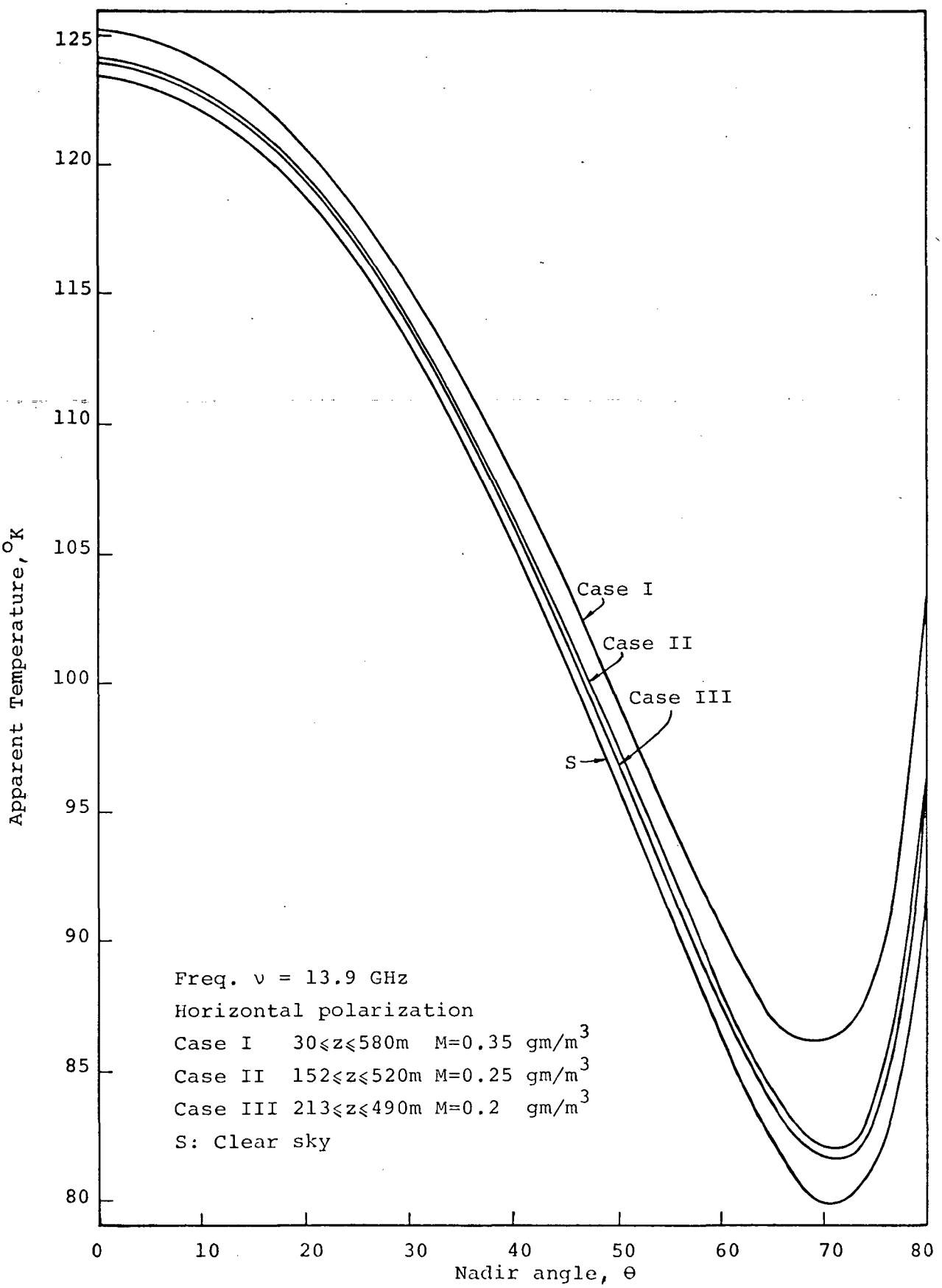

Figure 8. Neiburger's Stratus Cloud Model, T_a v.s. θ

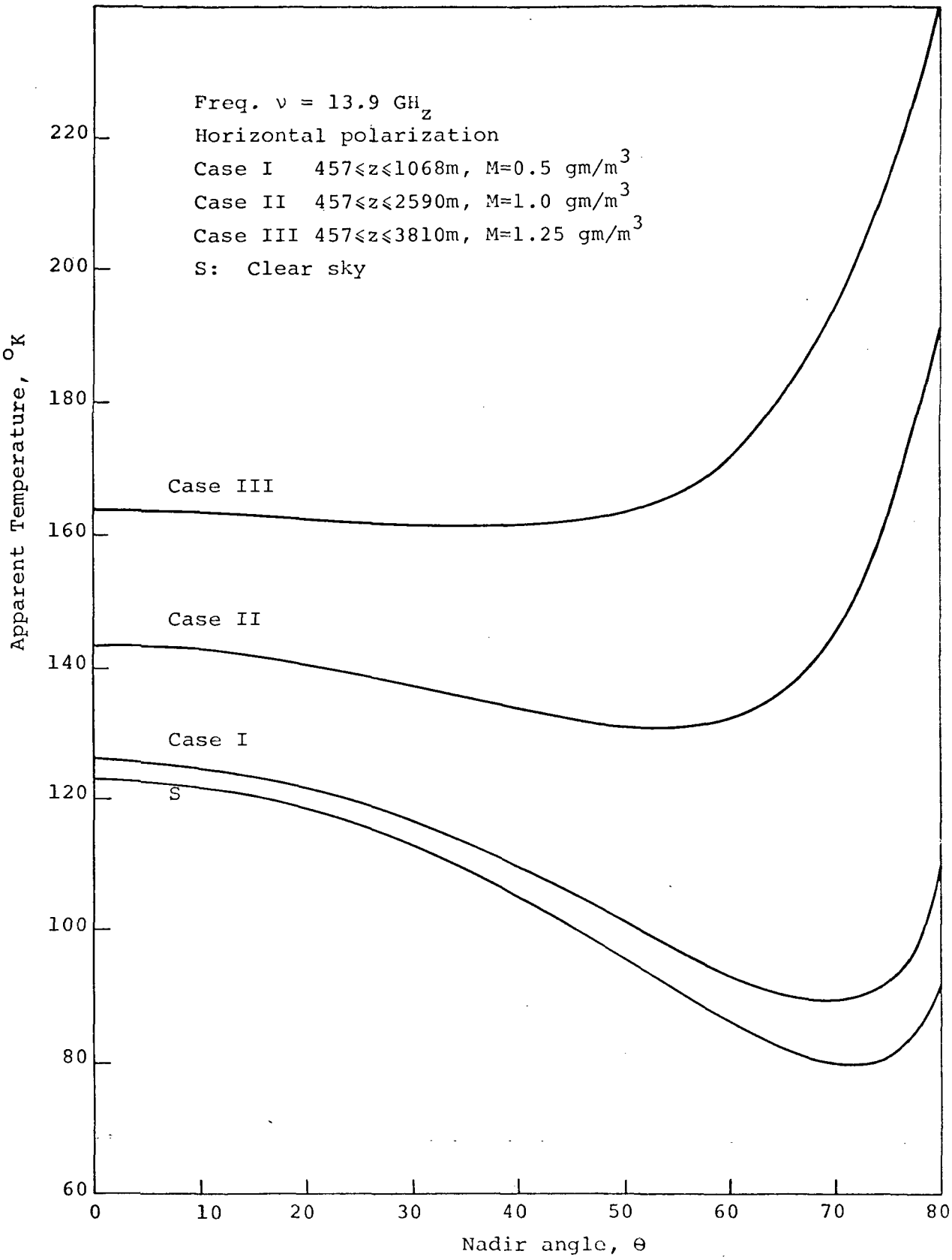

Figure 9. Levine's Cumulus Cloud Model T_a v.s. θ

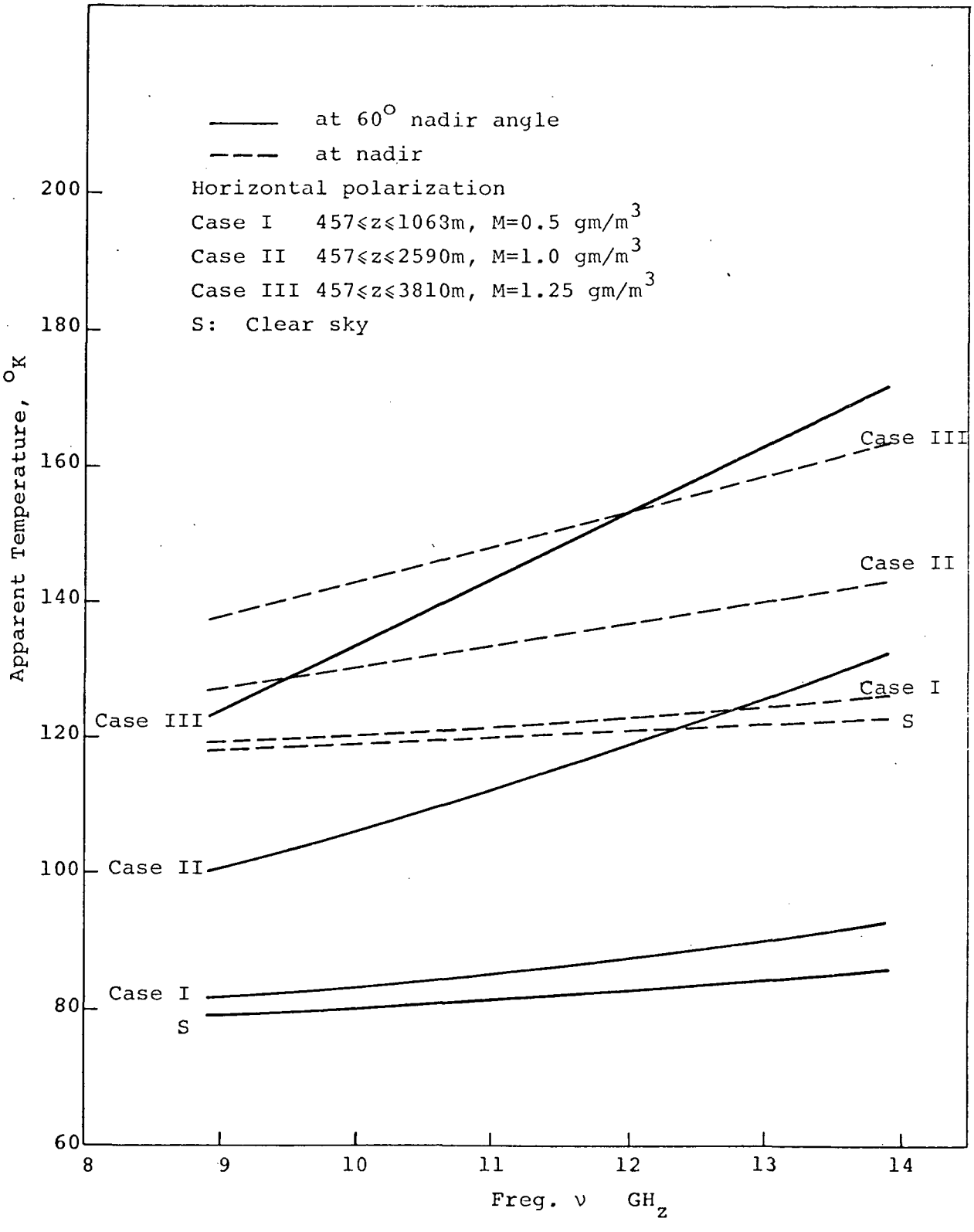

Figure 10. Levine's Cumulus Cloud Model, T_a v.s. ν

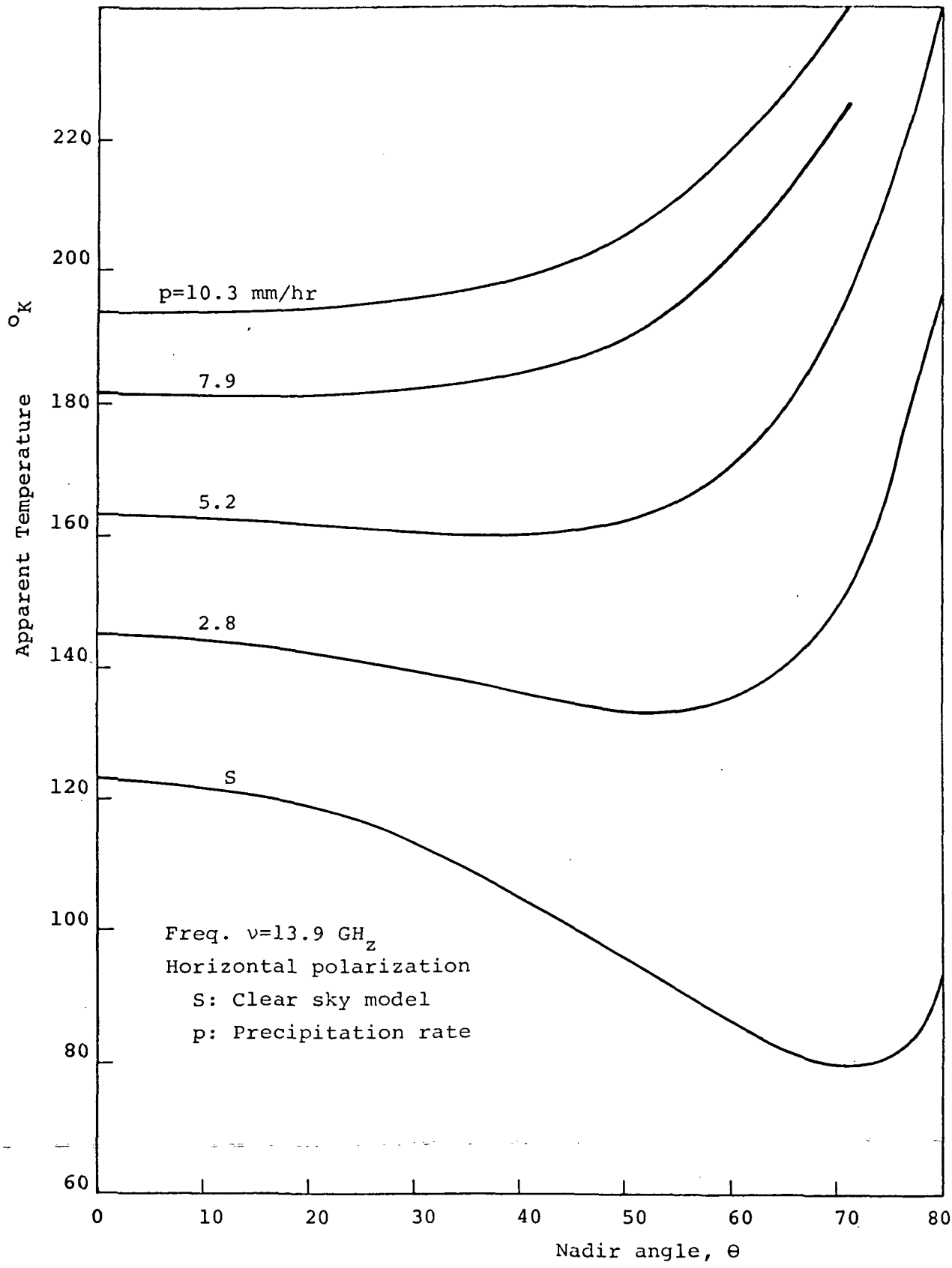

Figure 11. Valley's Rain Model Case I, T_a v.s. θ

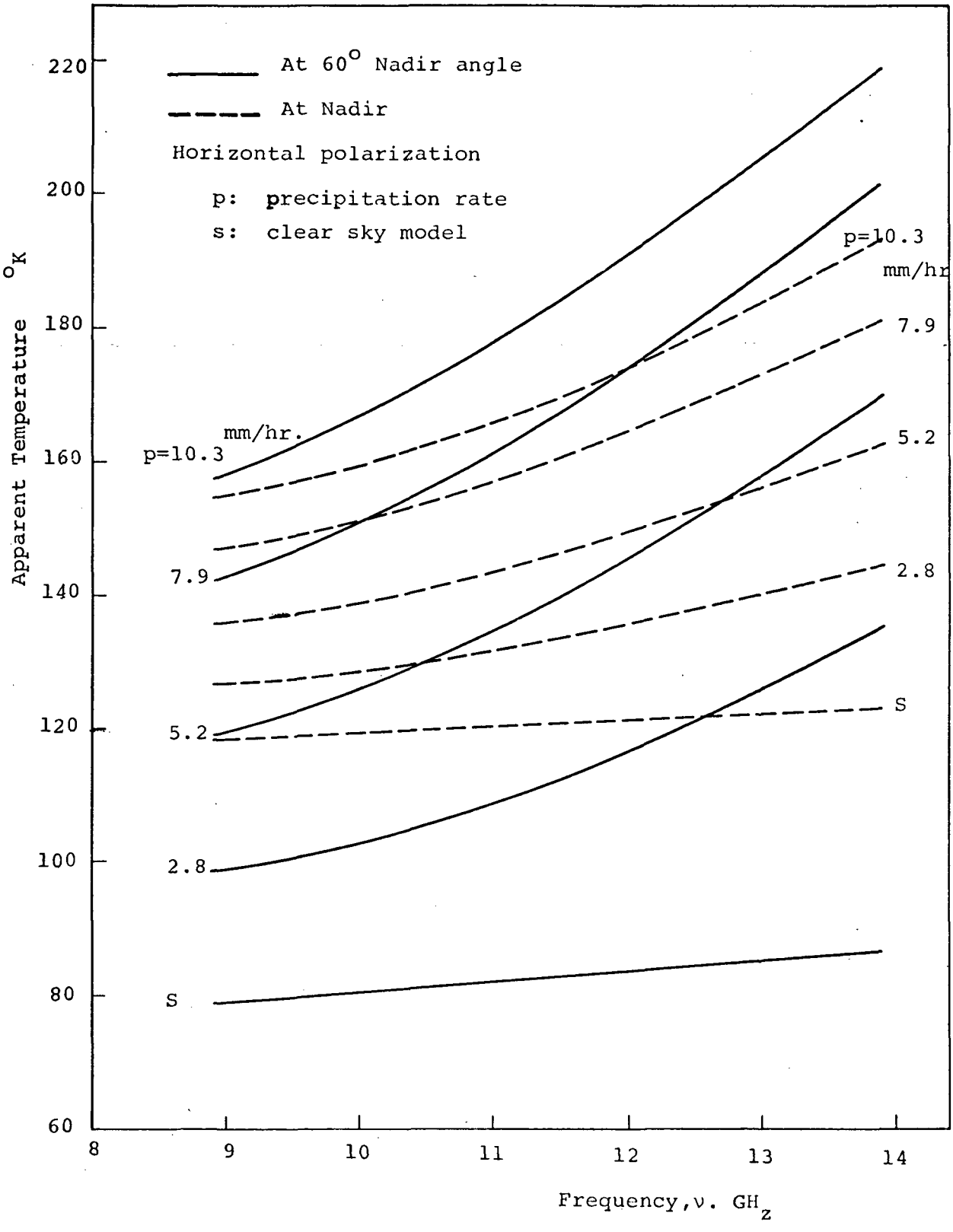

Fig.12 Valley's Rain Model Case I, T_a v.s. ν

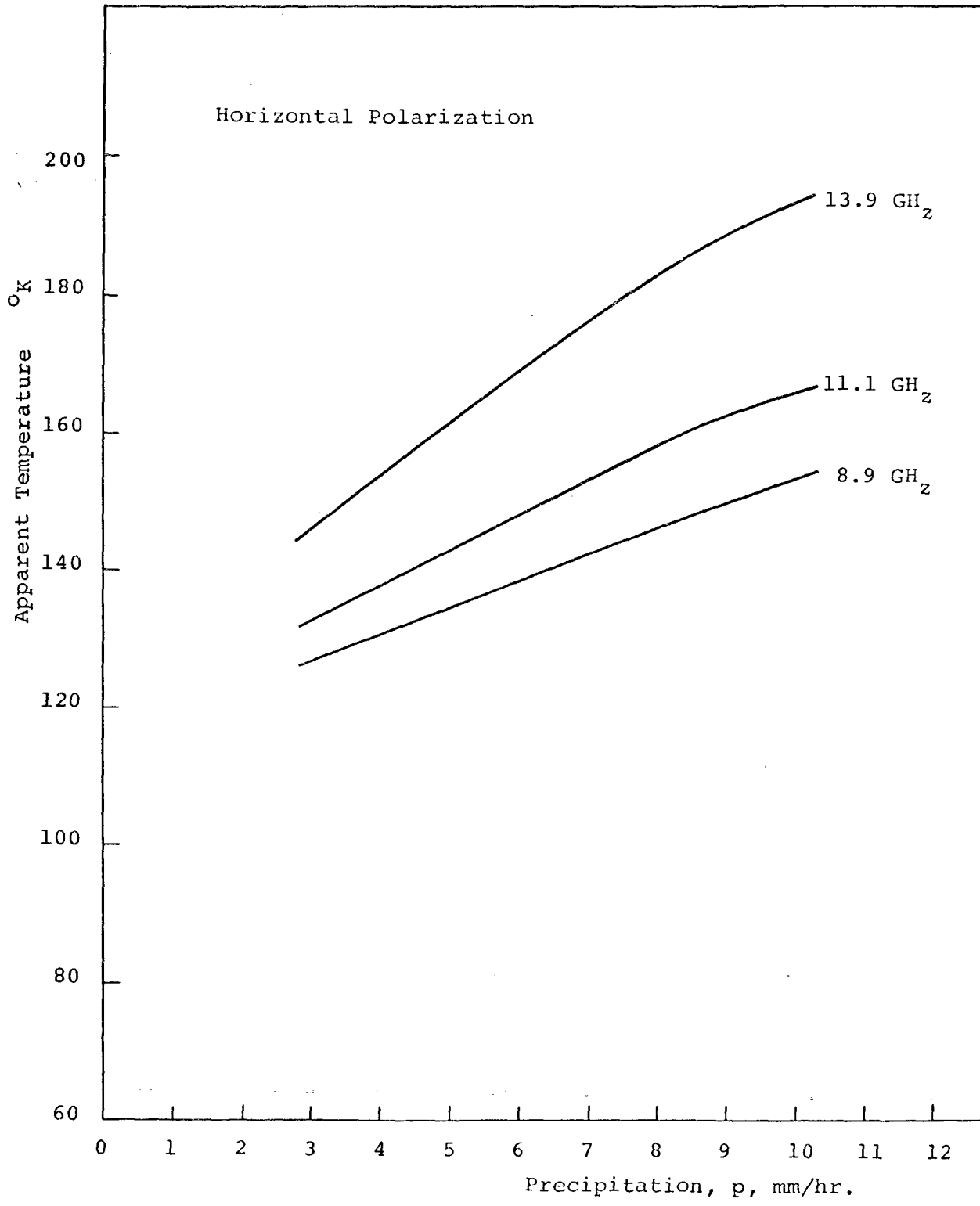

Fig. 13 Valley's Rain Model Case I, T_a v.s. p

APPENDIX A. SURFACE EMISSIVITY OF A SMOOTH SEA

$$\epsilon_j(\theta) = 1 - |R_j(\theta)|^2 \quad \text{where} \quad j = h \text{ or } v \tag{1}$$

$$R_h(\theta) = \frac{\cos\theta - \sqrt{\epsilon_r - \sin^2\theta}}{\cos\theta + \sqrt{\epsilon_r - \sin^2\theta}} \tag{2}$$

$$R_v(\theta) = \frac{\epsilon_r \cos\theta - \sqrt{\epsilon_r - \sin^2\theta}}{\epsilon_r \cos\theta + \sqrt{\epsilon_r - \sin^2\theta}} \tag{3}$$

where $$\epsilon_r = \epsilon_1 - j\epsilon_2 \tag{4}$$

let $$u = \cos\theta$$

and $$\sqrt{\epsilon_r - \sin^2\theta} = \sqrt{\epsilon_1 - j\epsilon_2 - (1-u^2)} = \sqrt{(\epsilon_1 + u^2 - 1) - j\epsilon_2} = p - jq \tag{5}$$

then squaring eq.(5):

$$(\epsilon_1 + u^2 - 1) - j\epsilon_2 = p^2 - q^2 - 2jpq \tag{6}$$

That is $$p^2 - q^2 = \epsilon_1 + u^2 - 1 \tag{7}$$

$$2pq = \epsilon_2 \tag{8}$$

Solving (7), (8) for p^2, and q^2 get

$$p^2 = \frac{1}{2}\left\{\left[(\epsilon_1 + u^2 - 1)^2 + \epsilon_2^2\right]^{1/2} + (\epsilon_1 + u^2 - 1)\right\} \tag{9}$$

$$q^2 = \frac{1}{2}\left\{\left[(\epsilon_1 + u^2 - 1)^2 + \epsilon_2^2\right]^{1/2} - (\epsilon_1 + u^2 - 1)\right\} \tag{10}$$

$R_h(\theta)$ and $R_v(\theta)$ then can be expressed in terms of u,p, and q as:

$$R_h(\theta) = \frac{u - p + jq}{u + p - jq} \tag{11}$$

$$R_v(\theta) = \frac{(\epsilon_1 - j\epsilon_2)u - (p - jq)}{(\epsilon_1 - j\epsilon_2)u + (p - jq)} = \frac{(u\epsilon_1 - p) - j(u\epsilon_2 - q)}{(u\epsilon_1 + p) - j(u\epsilon_2 + q)} \tag{12}$$

The surface emissivity have the following forms:

$$\epsilon_h(\theta) = 1 - |R_h(\theta)|^2 = 1 - R_h(\theta) R_h(\theta)^*$$

$$\approx 1 - \frac{(u-p)^2 + q^2}{(u+p)^2 + q^2}$$

$$\approx \frac{4up}{u^2 + 2up + (p^2+q^2)} \tag{13}$$

$$\epsilon_v(\theta) \approx 1 - |R_v(\theta)|^2 = 1 - R_v(\theta) R_v(\theta)^*$$

$$\approx 1 - \frac{(u\epsilon_1 - p)^2 + (u\epsilon_2 - q)^2}{(u\epsilon_1 + p)^2 + (u\epsilon_2 + q)^2}$$

$$\approx \frac{4u(\epsilon_1 p + \epsilon_2 q)}{(u\epsilon_1 + p)^2 + (u\epsilon_2 + q)^2}$$

$$\approx \frac{4u(\epsilon_1 p + \epsilon_2 q)}{u^2(\epsilon_1^2 + \epsilon_2^2) + 2u(\epsilon_1 p + \epsilon_2 q) + (p^2+q^2)} \tag{14}$$

let $$B \approx (p^2+q^2)^{1/2} = \left[(\epsilon_1 + u^2 - 1)^2 + \epsilon_2^2\right]^{1/4} . \tag{15}$$

then $$p \approx \sqrt{\tfrac{1}{2}\left[B^2 + (\epsilon_1 - \sin^2\theta)\right]} = B\sqrt{\tfrac{1}{2}\left(1 + \frac{\epsilon_1 - \sin^2\theta}{B^2}\right)} \tag{16}$$

and let $$\cos\psi = \frac{\epsilon_1 - \sin^2\theta}{B^2} \tag{17}$$

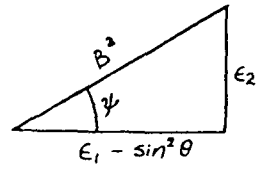

Fig. A-1

then from Figure A-1

$$\tan\psi \approx \frac{\epsilon_2}{\epsilon_1 - \sin^2\theta}$$

$$\psi \approx \tan^{-1}\left(\frac{\epsilon_2}{\epsilon_1 - \sin^2\theta}\right) \tag{18}$$

By trigonometric identity $\cos\frac{\psi}{2} = \sqrt{\frac{1}{2}(1+\cos\psi)}$

we finally get

$$P = B\cos\frac{\psi}{2} = B\cos\psi_0 \tag{19}$$

where

$$\psi_0 = \frac{\psi}{2} = \frac{1}{2}\tan^{-1}\left(\frac{\epsilon_2}{\epsilon_1 - \sin^2\theta}\right) \tag{20}$$

Hence

$$\epsilon_h(\theta) = \frac{4\cos\theta B\cos\psi_0}{\cos^2\theta + 2\cos\theta B\cos\psi_0 + B^2} \tag{21}$$

put

$$\psi_2 = \tan^{-1}\frac{\epsilon_2}{\epsilon_1}$$

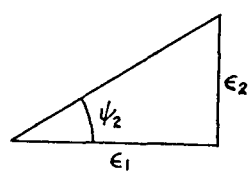

Fig. 2

then from fig. A-2

$$\epsilon_1 = \sqrt{\epsilon_1^2 + \epsilon_2^2}\cos\psi_2 \tag{22}$$

$$\epsilon_2 = \sqrt{\epsilon_1^2 + \epsilon_2^2}\sin\psi_2 \tag{23}$$

From (19) we get

$$P = B\cos\psi_0$$

and similarly

$$q = B\sqrt{\frac{1}{2}\left(1 - \frac{\epsilon_1 - \sin^2\theta}{B^2}\right)} = B\sqrt{\frac{1}{2}(1-\cos\psi)} = B\sin\frac{\psi}{2}$$
$$= B\sin\psi_0 \tag{24}$$

USING (22), (23), (24) and (19), we have

$$u(\epsilon_1 p + \epsilon_2 q) = u\sqrt{\epsilon_1^2+\epsilon_2^2}\, B(\cos\psi_2\cos\psi_0 + \sin\psi_2\sin\psi_0)$$
$$= GB\cos(\psi_2 - \psi_0) \tag{25}$$

where $$G = \cos\theta\,(\epsilon_1 + \epsilon_2)^{1/2} \tag{26}$$

Hence from eq.(14) get

$$\epsilon_v(\theta) = \frac{4GB\cos(\psi_2 - \psi_0)}{G^2 + 2GB\cos(\psi_2 - \psi_0) + S^2} \tag{27}$$

REFERENCES

1. Stogryn, A., "The Apparent Temperature of the Sea at Microwave Frequencies," IEEE Trans. on Antennas and Propagation, vol. AP-15, March 1967, pp. 278-286.

2. Fung, A. K. and F. T. Ulaby, "The Apparent Surface Temperature at Microwave Frequencies," Fall URSI Meeting, Austin, Texas, December 8-10, 1969.

3. Valley, S. L.,"Handbook of Geophysics and Space Environment," McGraw-Hill Book Company, New York, 1965.

4. Van Vleck, J. H. and V. F. Weisskopf, "On the Shape of Collision Broadened Lines," Reviews of Modern Physics, vol. 17, 1945.

5. Meeks, M. L. and A. E. Lilley, "The Microwave Spectrum of Oxygen in the Earth's Atmosphere," JGR, vol. 68, 20.6, 1963, pp. 1683.

6. Barrett, A. H. and V. K. Chung, "A Method for the Determination of High-Altitude Water-Vapor Abundance from Ground-Based Microwave Observations," JGR, vol. 67, no. 11, 1962, pp. 4259.

7. Ulaby, F. T. and A. W. Straiton, "Atmospheric Absorption of Radio Waves between 150 and 350 GHz," IEEE Trans. Antenna and Propagation, July 1970.

8. Ryde, J. W., and D. Ryde, "Attenuation of Centimeters Waves by Rain, Hail and Clouds," Rept. 8516, General Electric Company Research Labs, Wembley, England, August 1944.

9. Gunn, K. L. S. and T. W. R. Gast, "The Microwave Properties of Precipitation Particles," Quarterly Jour. of the Royal Met. Soc., vol. 80, no. 346, October 1954, pp. 522-545.

10. Benoit, Andre, "Signal Attenuation Due to Neutral Oxygen and Water Vapor, Rain, and Clouds," The Microwave Journal, vol. 11, no. 11, November 1968, pp. 73-80.

11. Holzer, W.,"Atmospheric Attenuation is Satellite Communications," The Microwave Journal, vol. 8, no. 3, March 1965, pp. 119-125.

12. Medhurst, R. G., "Rainfall Attenuation of Centimeter Waves: Comparison of Theory and Measurement," IEEE Trans. on Antenna and Propagation, vol. AP-13, July 1965, pp. 550-564.

13. Goldstein, H., "Attenuation by Condensed Water, Propagation of Short Radio Waves," McGraw-Hill Book Co., New York, 1951, pp. 671-692.

14. Haroules, G. G. and W. E. Brown, IV., "The Simultaneous Investigation of Attenuation and Emission by the Earth's Atmosphere at Wavelengths from 4 cm to 8 mm," JGR, vol. 74, no. 18, August 20, 1969, pp. 4453-4471.

15. Kreiss, W. T., "Meteorological Observations with Passive Microwave Systems," Ph. D. Dissertation, The Department of Atmospheric Sciences, University of Washington, Seattle, Washington, February 1968.

16. Kreiss, W. T., "The Influence of Clouds on Microwave Brightness Temperatures Viewing Downward over open seas," Proc. IEEE, vol. 57, no. 4, April 1969.

17. Paris, J. F., "Microwave Radiometry and Its Applications to Marine Meteorology and Oceanography," Ph. D. Dissertation, Texas A & M University, Dept. of Oceanography, January 1969.

18. Porter, R. A., "An Analytical Study of Measured Radiometric Data," vol. I, April 1970.

19. Mie, G., "Beitrage zur Optik truber Medien, speziell kolloidaler Metallosungen, Ann. Phys., vol. 25, 1908, pp. 377-345.

20. Donn, W. L., "Meteorology," 3rd ed., McGraw-Hill, New York, pp. 107.

21. Malkus, J. S., "Some Results of a Trade-Cumulus Cloud Investigation," J. of Meteor., vol.11, no. 3, June 1954.

22. Spyers-Duran, P. A., "Comparative Measurements of Cloud Liquid Water Using Heated Wire and Cloud Replicating Devices," J. of Appl. Meteor., vol. 7, August 1968, pp. 674-678.

23. Levine, J., "The Dynamics of Cumulus Convection in the Trades A Combined Observational and Theoretical Study," Woods Hole Oceanographic Institution, Ref. no. 65-43, August 1965.

24. Neiburger, M., "Reflection, Absorption, and Transmission of Insolation by Stratus Cloud," J. of Meteor., vol. 6, no. 2, April 1949.

25. Aufm Kampe, H. J. and Weickmann, "Visibility and liquid Water Content in Clouds in the Free Atmosphere," J. of Meteor., vol. 7, no. 1, February 1950.

26. Ippolito, L.J., "Millimeter Wave Propagation Measurements from the Applications Technology Satellite (ATS-V) IEEE Trans. on Antennas and Propagation, vol. AP-18, no. 4, July 1970.

NATIONAL AERONAUTICS AND SPACE ADMINISTRATION
WASHINGTON, D.C. 20546

OFFICIAL BUSINESS
PENALTY FOR PRIVATE USE $300

SPECIAL FOURTH-CLASS RATE BOOK

POSTAGE AND FEES PAID
NATIONAL AERONAUTICS AND SPACE ADMINISTRATION
451

U.S.MAIL

POSTMASTER: If Undeliverable (Section 158 Postal Manual) Do Not Return

"The aeronautical and space activities of the United States shall be conducted so as to contribute . . . to the expansion of human knowledge of phenomena in the atmosphere and space. The Administration shall provide for the widest practicable and appropriate dissemination of information concerning its activities and the results thereof."

—NATIONAL AERONAUTICS AND SPACE ACT OF 1958

NASA SCIENTIFIC AND TECHNICAL PUBLICATIONS

TECHNICAL REPORTS: Scientific and technical information considered important, complete, and a lasting contribution to existing knowledge.

TECHNICAL NOTES: Information less broad in scope but nevertheless of importance as a contribution to existing knowledge.

TECHNICAL MEMORANDUMS: Information receiving limited distribution because of preliminary data, security classification, or other reasons. Also includes conference proceedings with either limited or unlimited distribution.

CONTRACTOR REPORTS: Scientific and technical information generated under a NASA contract or grant and considered an important contribution to existing knowledge.

TECHNICAL TRANSLATIONS: Information published in a foreign language considered to merit NASA distribution in English.

SPECIAL PUBLICATIONS: Information derived from or of value to NASA activities. Publications include final reports of major projects, monographs, data compilations, handbooks, sourcebooks, and special bibliographies.

TECHNOLOGY UTILIZATION PUBLICATIONS: Information on technology used by NASA that may be of particular interest in commercial and other non-aerospace applications. Publications include Tech Briefs, Technology Utilization Reports and Technology Surveys.

Details on the availability of these publications may be obtained from:

SCIENTIFIC AND TECHNICAL INFORMATION OFFICE

NATIONAL AERONAUTICS AND SPACE ADMINISTRATION

Washington, D.C. 20546